

# PASSIVITY-BASED NONLINEAR STABILIZING CONTROL FOR A MOBILE INVERTED PENDULUM

Kazuto Yokoyama and Masaki Takahashi

Keio University, 3-14-1 Hiyoshi, Kohoku-ku, 223-8522, Yokohama, Japan

**Keywords:** Passivity, Nonlinear Control, Interconnection and Damping Assignment, Mobile Inverted Pendulum, Experiment.

**Abstract:** Mobile inverted pendulums (MIPs) need to be stabilized at all times using a reliable control method. Previous studies were based on a linearized model or feedback linearization. In this study, interconnection and damping assignment passivity-based control (IDA-PBC) is applied. The IDA-PBC is a nonlinear control method which has been shown to be powerful in stabilizing underactuated mechanical systems. Although partial differential equations (PDEs) must be solved to derive the IDA-PBC controller and this is a difficult task in general, we show that the IDA-PBC controller for the MIP can be derived solving the PDEs. We also formulate conditions which must be satisfied to guarantee asymptotic stability and show a procedure to estimate the domain of attraction. Simulation results indicate that the IDA-PBC controller achieves fast performance theoretically ensuring a large domain of attraction. We also verify its effectiveness in experiments. In particular control performance under an impulsive disturbance to the MIP are verified. The IDA-PBC achieves as fast transient performance as a linear-quadratic regulator (LQR). In addition, we show that even when the pendulum declines quickly and largely because of the disturbance, the IDA-PBC controller is able to stabilize it whereas the LQR can not.

## 1 INTRODUCTION

A mobile inverted pendulum (MIP), as shown in Figure 1, has a small footprint and can turn in a small radius. The MIP is used as a basic model of personal mobility devices such as Segway. The MIP needs to be stabilized at all times using a reliable control method. Previous studies were based on a linearized model (Grasser et al., 2002) (Matsumoto et al., 1993). Other typical approaches use feedback linearization (Pathak et al., 2005). However, the former methods can not guarantee stability when the MIP declines quickly and largely, and the latter ones require exact parameters of the MIP. These methods can be inadequate when parameters are uncertain.

In this study we have focused on the MIP in a two-dimensional sagittal plane in order to design a nonlinear controller that guarantees large domain of attraction without using a linearized model or feedback linearization. This will lead to safe and reliable operation of the system. For this purpose, we applied a nonlinear control method called interconnection and damping assignment

passivity- based control (IDA-PBC) (Ortega et al., 2002a) to the MIP. This control method shapes the total energy preserving port-Hamiltonian (PH) structure (van der schaft, 1999) of the system. Then stabilization is achieved utilizing passivity of the PH system.

Passivity is an essential energetic property of physical systems. In general, control methods

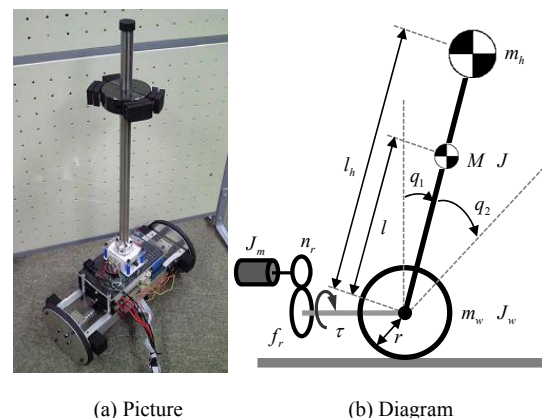


Figure 1: The mobile inverted pendulum.

utilizing passivity are expected to be robust (Ortega et al., 2001). In addition, the IDA-PBC has been shown to be powerful in stabilizing underactuated mechanical systems (Gómez-Estern et al., 2001) (Ortega et al., 2002b) (Acosta et al., 2005) such as a cart-inverted pendulum.

To derive the IDA-PBC controller, partial differential equations (PDEs) must be solved. This is a difficult task in general. A previous study showed a constructive solution of the PDEs under several assumptions and applied the solution to a cart-inverted pendulum (Acosta et al., 2005). However, the MIP does not satisfy these assumptions, and thus, it is still necessary to solve the PDEs.

We show that the PDEs for the MIP can be solved without using the constructive solution. We also formulate conditions to guarantee asymptotic stability and also show a procedure to estimate the domain of attraction. Although in one study an IDA-PBC controller was derived for a three-dimensional MIP, only the pendulum angle was stabilized (Muralidharan et al., 2009). The stability of the other states was not considered, and the procedure to solve the PDEs was different from this study.

The effectiveness of the proposed controller is verified in simulations and experiments.

## 2 MODELING

A diagram of the MIP is shown in Figure 1(b). The physical parameters of the experimental MIP are shown in Table 1. We ignore the friction and a slip between the wheel and the ground.  $q_1$  is the pendulum angle from the vertical line and  $q_2$  is the relative wheel angle with respect to the pendulum body.  $\mathbf{q} = [q_1 \ q_2]^T$  is the generalized position vector and  $g$  is the gravity acceleration. Equations of motion are derived based on a previous study (Matsumoto et al., 1993). They can be represented as a PH system (van der shaft, 1999).

$$\begin{bmatrix} \dot{\mathbf{q}} \\ \dot{\mathbf{p}} \end{bmatrix} = \begin{bmatrix} \mathbf{0} & \mathbf{I}_2 \\ -\mathbf{I}_2 & \mathbf{0} \end{bmatrix} \begin{bmatrix} \nabla_{\mathbf{q}} H \\ \nabla_{\mathbf{p}} H \end{bmatrix} + \begin{bmatrix} \mathbf{0} \\ \mathbf{G} \end{bmatrix} u \quad (1)$$

$$H(\mathbf{q}, \mathbf{p}) = \frac{1}{2} \mathbf{p}^T \mathbf{M}^{-1}(\mathbf{q}) \mathbf{p} + V(\mathbf{q}) \quad (2)$$

$$\mathbf{M} = \begin{bmatrix} 2a \cos q_1 + b & a \cos q_1 + c \\ a \cos q_1 + c & 1 \end{bmatrix} \quad (3)$$

Table 1: Parameters of the mobile inverted pendulum.

| Parameter | Unit  | Value                |
|-----------|---|----------------------|
| $M$       | kg  | 2.3                  |
| $m_w$     | kg  | 0.63                 |
| $m_h$     | kg  | 1.0                  |
| $J$       | $\text{kg} \cdot \text{m}^2$                        | $1.9 \times 10^{-2}$ |
| $J_w$     | $\text{kg} \cdot \text{m}^2$                        | $1.8 \times 10^{-3}$ |
| $J_m$     | $\text{kg} \cdot \text{m}^2$                        | $2.1 \times 10^{-6}$ |
| $l$       | m   | 0.061                |
| $l_h$     | m   | 0.50                 |
| $r$       | m   | 0.075                |
| $n_r$     | -   | 50                   |
| $f_r$     | $\text{N} \cdot \text{m} \cdot \text{s}/\text{rad}$ | 0                    |

$$V(q_1) = e \cos q_1 \quad (4)$$

$$\mathbf{G} = [0 \ 1]^T \quad (5)$$

$$d = (M + m_h + m_w)r^2 + J_w + n_r^2 J_m \quad (6)$$

$$a = \frac{1}{d} (Ml + m_h l_h) r \quad (7)$$

$$b = \frac{1}{d} \{ (M + m_h + m_w)r^2 + Ml^2 + m_h l_h^2 + J + J_w \} \quad (8)$$

$$c = \frac{1}{d} \{ (M + m_h + m_w)r^2 + J_w \} \quad (9)$$

$$e = \frac{g}{d} (Ml + m_h l_h) \quad (10)$$

$$u = \frac{\tau}{d} \quad (11)$$

$H$  and  $V$  are the total and potential energy of the open-loop PH system respectively.  $\mathbf{p} = \mathbf{M}\dot{\mathbf{q}}$  is the generalized momenta. In this study, we consider the MIP in the upper half plane  $q_1 \in (-\pi/2, \pi/2)$ .

## 3 DRIVATION OF CONTROLLER

### 3.1 IDA-PBC

The IDA-PBC controller for frictionless underactuated mechanical systems is obtained solving the PDEs (Ortega et al., 2002b)

$$\mathbf{G}^\perp \left\{ \nabla_{\mathbf{q}} (\mathbf{p}^T \mathbf{M}^{-1} \mathbf{p}) - \mathbf{M}_d \mathbf{M}^{-1} \nabla_{\mathbf{q}} (\mathbf{p}^T \mathbf{M}_d^{-1} \mathbf{p}) + 2\mathbf{J}_2 \mathbf{M}_d^{-1} \mathbf{p} \right\} = \mathbf{0} \quad (12)$$

$$\mathbf{G}^\perp \left\{ \nabla_{\mathbf{q}} V - \mathbf{M}_d \mathbf{M}^{-1} \nabla_{\mathbf{q}} V_d \right\} = \mathbf{0} \quad (13)$$

where  $\mathbf{J}_2(\mathbf{q}, \mathbf{p}) \in \mathbb{R}^{n \times n}$  is a skew-symmetric matrix,  $\mathbf{G}^\perp \in \mathbb{R}^{m \times n}$  is a full rank left annihilator of  $\mathbf{G}$  and  $\text{rank}(\mathbf{G}^\perp) = n - m$ .  $\mathbf{M}_d$  and  $V_d$  are desired inertia matrix and potential energy of a closed-loop PH system respectively. Consider we can obtain the solution of the PDEs, then the IDA-PBC control input is represented as follows.

$$\mathbf{u} = \mathbf{u}_{es} + \mathbf{u}_{di} \quad (14)$$

$$\mathbf{u}_{es} = (\mathbf{G}^T \mathbf{G})^{-1} \mathbf{G} (\nabla_{\mathbf{q}} H - \mathbf{M}_d \mathbf{M}^{-1} \nabla_{\mathbf{q}} H_d + \mathbf{J}_2 \mathbf{M}_d^{-1} \mathbf{p}) \quad (15)$$

$$\mathbf{u}_{di} = -\mathbf{K}_d \mathbf{G}^T \nabla_{\mathbf{p}} H_d \quad (16)$$

$\mathbf{u}_{es}$  shapes the total energy of the system.  $\mathbf{u}_{di}$  is used for achieving asymptotic stability. It is a negative feedback of the passive output  $\mathbf{y}_c = \mathbf{G}^T \nabla_{\mathbf{p}} H_d$  of the closed-loop PH system and called damping injection.  $\mathbf{K}_d > 0$  is a constant matrix.  $H_d$  is the total energy of the closed-loop PH system and can be represented replacing  $\mathbf{M}$  and  $V$  in (2) with  $\mathbf{M}_d$  and  $V_d$  respectively. The closed-loop PH system is represented as

$$\begin{bmatrix} \dot{\mathbf{q}} \\ \dot{\mathbf{p}} \end{bmatrix} = \begin{bmatrix} \mathbf{0} & \mathbf{M}^{-1} \mathbf{M}_d \\ -\mathbf{M}_d \mathbf{M}^{-1} & \mathbf{J}_2 \end{bmatrix} \begin{bmatrix} \nabla_{\mathbf{q}} H_d \\ \nabla_{\mathbf{p}} H_d \end{bmatrix} + \begin{bmatrix} \mathbf{0} \\ \mathbf{G} \end{bmatrix} \mathbf{u}_{di} \quad (17)$$

Let  $\mathbf{q}^*$  be a desired equilibrium. If  $\mathbf{M}_d$  is positive definite in the neighbourhood of  $\mathbf{q} = \mathbf{q}^*$  and

$$\mathbf{q}^* = \arg \min V_d(\mathbf{q}) \quad (18)$$

is satisfied, then the point  $(\mathbf{q}^*, \mathbf{0})$  is a stable equilibrium of the closed-loop system with a Lyapunov function  $H_d$ . In addition, if the closed-loop PH system is zero-state detectable, then the desired equilibrium  $(\mathbf{q}^*, \mathbf{0})$  is asymptotically stable.

### 3.2 Simplifying PDEs

In this study, a method to simplify the PDEs for a class of systems (Gómez-Estern et al., 2001) (Ortega et al., 2002b) is utilized to solve the PDEs and derive the controller. Three assumptions are required.

Assumption 1:  $m = n - 1$

Under this condition  $\mathbf{G}^\perp = \mathbf{e}_k^T$  and  $k$  is a natural number which accounts for the underactuated coordinate and  $\mathbf{e}_k$  is a vector with all zeros except the  $k$ -th element which equals 1.

Assumption 2 and 3:  $\mathbf{M}$  and  $\mathbf{M}_d$  depend only on the underactuated coordinate respectively.

Under these assumptions, the PDE (12) can be simplified to ordinary differential equations (ODEs).

$$\frac{dm_{d2}}{dq_1} = \frac{-a \{ 2(a \cos q_1 + c - 1) m_{d1} m_{d2} + (-a^2 \cos^2 q_1 - 2ac \cos q_1 - c^2 + 2c - b) (m_{d1} m_{d3} + m_{d2}^2) + (2a^2 \cos^2 q_1 + 2ab \cos q_1 - 2c^2 + 2bc) m_{d2} m_{d3} \}}{\det(\mathbf{M}) \{-m_{d1} + (a \cos q_1 + c) m_{d2}\}} \sin q_1 \quad (23)$$

$$\frac{d}{dq_k} (\mathbf{M}_d)_{(i,k)} = -\frac{1}{(\mathbf{M}_d \mathbf{M}^{-1})_{(k,k)}} \left( \mathbf{M}_d \frac{d}{dq_k} (\mathbf{M}^{-1}) \mathbf{M}_d \right)_{(i,k)} \quad (19)$$

The subscript  $(i, j)$  represents the  $i$ - $j$  element of the matrix. These ODEs are defined only when the next condition is satisfied.

$$(\mathbf{M}_d \mathbf{M}^{-1})_{(k,k)} (\dot{q}_k^*) \neq 0 \quad (20)$$

### 3.3 Solutions of PDEs

First, we solve ODEs (19). The assumptions 1 and 2 are clearly satisfied because  $n = 2$ ,  $m = 1$  and  $k = 1$ . Considering the third assumption, we set  $\mathbf{M}_d$  as

$$\mathbf{M}_d(q_1) = \begin{bmatrix} m_{d1}(q_1) & m_{d2}(q_1) \\ m_{d2}(q_1) & m_{d3}(q_1) \end{bmatrix} \quad (21)$$

The ODE is written as (22) and (23)

$$\frac{dm_{d1}}{dq_1} = \frac{-2a \{ (-a \cos q_1 - c + 1) m_{d1} + (a \cos q_1 + b - c) m_{d2} \}}{\det(\mathbf{M})} \sin q_1 \quad (22)$$

Although the equations of motion of the MIP are different from those of the cart-inverted pendulum, the structure of the above ODEs is similar to that of the previous study (Gómez-Estern et al., 2001). Focusing on that the right-hand sides of the ODEs are the first degree with respect to the elements of  $\mathbf{M}_d$ , we set  $m_{d2}$  and  $m_{d3}$  as

$$m_{d2}(q_1) = \alpha_2(q_1) m_{d1}(q_1) \quad (24)$$

$$m_{d3}(q_1) = \alpha_3(q_1) m_{d1}(q_1) \quad (25)$$

$\alpha_2$  and  $\alpha_3$  are scalar functions of  $q_1$  and must be designed to satisfy the conditions for stability. The solution of the ODE (22) can be written as

$$m_{d1}(q_1) = K_m e^{\int_{q_1}^{\alpha} F(\mu) d\mu} \quad (26)$$

$$F(q_1) = \frac{-2a \{ \alpha_2 (a \cos q_1 + b - c) - a \cos q_1 - c + 1 \}}{\det(\mathbf{M})} \sin q_1 \quad (27)$$

where  $K_m > 0$  is a constant parameter and  $q_1^*$  is the desired equilibrium of the pendulum angle and  $q_1^* = 0$  in this study. In summary, first we design  $m_{d2}$  by setting  $\alpha_2$ , then  $\alpha_3$  (at the same time  $m_{d3}$ ) is obtained from the ODE (23). Therefore, we must find  $\alpha_2$  which satisfy the conditions for stability.

Second, we solve the potential energy PDE (13). The solution of this equation is written as  $\Phi$  is an arbitrary differentiable function.

Using  $\mathbf{M}_d$  and  $V_d$  obtained from the above

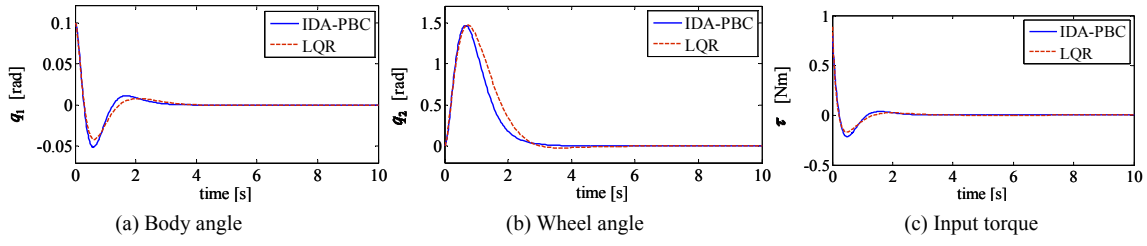


Figure 2: Regulator performance of IDA-PBC and LQR.

$$V_d(\mathbf{q}) = \int_0^{q_1} \frac{1}{(\mathbf{M}_d \mathbf{M}^{-1})_{(1,1)}(\mu)} \frac{\partial V}{\partial q_1}(\mu) d\mu + \Phi(z(\mathbf{q})) \quad (28)$$

$$z(\mathbf{q}) \triangleq q_2 - \int_0^{q_1} \frac{(\mathbf{M}_d \mathbf{M}^{-1})_{(1,2)}(\mu)}{(\mathbf{M}_d \mathbf{M}^{-1})_{(1,1)}(\mu)} d\mu \quad (29)$$

procedure, the IDA-PBC control input is calculated from (14) to (16) where

$$\mathbf{J}_2 = \begin{bmatrix} 0 & -j_2 \\ j_2 & 0 \end{bmatrix} \quad (30)$$

$$J_{22} = \frac{1}{2} \mathbf{p}^T \left\{ \frac{d\mathbf{M}^{-1}(q_1)}{dq_1} - \mathbf{G}^T \mathbf{M}_d \mathbf{M}^{-1}(\mathbf{G}^T)^T \frac{d\mathbf{M}_d^{-1}(q_1)}{dq_1} \right\} \mathbf{M}_d \mathbf{e}_2 \quad (31)$$

## 4 CONDITIONS FOR STABILITY

The IDA-PBC controller is derived by designing  $\alpha_2$ . However, we must consider the conditions for stability and controller performance at the same time. We formulate  $\alpha_2$  which satisfies the conditions to avoid the complex task. We must consider three conditions:  $\mathbf{M}_d(q_1) > 0$ , (18) and (20). The condition (20) for  $V_d$  can be interpreted as

$$\nabla_{\mathbf{q}} V_d(\mathbf{q}^*) = 0 \quad (32)$$

$$\nabla_{\mathbf{q}}^2 \Phi(\mathbf{q}^*) > 0 \quad (33)$$

$$\frac{\partial^2 V_{d1}}{\partial^2 q_1}(q_1^*) > 0 \quad (34)$$

$V_{d1}$  is the first term of  $V_d$ . The conditions (32) and (33) are satisfied (Gómez-Estern et al., 2001) (Acosta et al., 2005) (Ortega et al., 2002b) with

$$\Phi(z(\mathbf{q})) = \frac{P}{2} \{z(\mathbf{q}) - z(\mathbf{q}^*)\}^2 \quad (35)$$

where  $P > 0$  is a constant parameter. (34) is calculated as  $1/(\mathbf{M}_d \mathbf{M}^{-1})_{(1,1)}(q_1^*) < 0$  and equivalent to

$$\alpha_2(q_1^*) > \frac{1}{a \cos q_1^* + c} > 0 \quad (36)$$

For simplicity and useful tuning of  $\alpha_2$ , we set

$$\alpha_2(q_1) = \frac{1}{\beta_1 \cos q_1 + \beta_2} \quad (37)$$

where  $\beta_1$  and  $\beta_2$  are constants. With this parameterization and after lengthy calculation, the all three conditions for stability are represented as

$$\beta_2 < -\cos q_1^* \cdot \beta_1 + a \cos q_1^* + c \quad (38)$$

$$\beta_2 > -\cos q_1^* \cdot \beta_1 \quad (39)$$

$$\beta_1 < 0 \quad (40)$$

$$\beta_2 < -\cos q_1^* \cdot \beta_1 + \frac{2\{a \cos q_1^* (a \cos q_1^* + b) + c(b - c)\}}{(a \cos q_1^* + c)^2 + (b - 2c)} \quad (41)$$

Consequently, if we select  $\beta_1$  and  $\beta_2$  from the region characterized by the inequalities, then  $\mathbf{q} = \mathbf{q}^*$  is the isolated minimum of  $V_d$  and  $(\mathbf{q}^*, \mathbf{0})$  is stable. In addition, we can check  $y_c \equiv 0, u_{di} \equiv 0 \Rightarrow (\mathbf{q}, \dot{\mathbf{q}}) \rightarrow (\mathbf{q}^*, \mathbf{0})$  with lengthy calculation. Therefore the desired equilibrium is asymptotically stable at least in the neighbourhood of  $q_1 = q_1^*$ .

An estimate of the domain of attraction can be calculated evaluating the conditions at general  $q_1 \in (-\pi/2, \pi/2)$ . Although we can not show the detailed procedure because of the paper space, the domain can be simply calculated solving

$$\beta_2 = -\cos q_{1\lim} \cdot \beta_1 + a \cos q_{1\lim} + c \quad (42)$$

for  $q_{1\lim}$ .  $H_d$  is a radially unbounded function on the set  $(-q_{1\lim}, q_{1\lim}) \times \mathbb{R}^3$  and this is the domain.

## 5 SIMULATION

The parameters of the IDA-PBC controller are as follows:  $K_m = 50$ ,  $\beta_1 = -2.3$ ,  $\beta_2 = 4.1$ ,  $P = 0.35$  and  $K_d = 45$ . The estimate of the domain of attraction is calculated as  $|q_1| < 0.590$ . An optimal feedback gain of the LQR controller is  $\mathbf{F}_{LQR} = [-303 \quad -3.38 \quad -65.8 \quad -4.26]$  with respect to a state vector  $\mathbf{x} = [q_1 \quad q_2 \quad \dot{q}_1 \quad \dot{q}_2]^T$ . These

parameters are selected by trial and error so that regulator performance of the controllers are similar in simulations. Although a large LQR gain will realize a large domain of attraction, the MIP became sensitive to sensor noise and we considered it. The simulation results with the initial state  $x_0 = [0.1 \ 0 \ 0 \ 0]^T$  and the desired wheel angle  $q_2^* = 0$  are shown in Figure 2. Although we can theoretically design an IDA-PBC controller with a larger estimate of the domain of attraction such as  $|q_1| < \pi/2$ , the transient performance tends to be slow.

We utilized knowledge of the trade-off between performance and the domain (Yokoyama & Takahashi, 2010) when we tune the IDA-PBC.

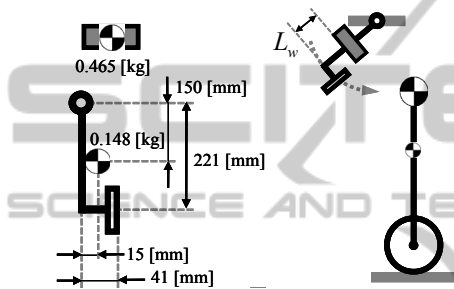


Figure 3: The equipment for adding disturbance.

## 6 EXPERIMENT

The angular velocity  $\dot{q}_1$  was measured with a gyro sensor, and the angle  $q_1$  is calculated integrating  $\dot{q}_1$ . We measured angles and angular velocities of the wheels with encoders, and the average values were respectively used as  $q_2$  and  $\dot{q}_2$ . An additional friction compensation torque was added. The friction was assumed to be Coulomb-type (Matsumoto et al., 1993). A diagram of the experimental setup is shown in Figure 3. We added the impulsive disturbance to the pendulum and compared the performance of the

IDA-PBC and LQR. The disturbance was realized using an arm hung from a fixed rotational axis. We lifted the arm to a fixed height and let it go softly, allowing the arm to collide with the pendulum. We adjusted the amplitude of the disturbance by changing  $L_w$  in Figure 3. The smaller the  $L_w$  was, the larger the disturbance became. The experiments were conducted under three cases of disturbance ( $L_w = 190, 80$  and  $40$  mm); we refer to these as Cases 1, 2 and 3 respectively.

The results are shown in Figure 4. In Case 1, which corresponds to the smallest disturbance, the both controllers performed similarly. In Case 2, the IDA-PBC showed slightly faster performance. In Case 3, which corresponds to the largest disturbance, only the IDA-PBC stabilized the MIP. Enlarged time histories of Case 3 are in Figure 5. Before the yellow shaded region, both controllers show similar time histories. However in the region, differences appear in the pendulum angles and input torque between the controllers. They gradually expand, and eventually the MIP with the LQR fell over. The system became unstable because of the pendulum angle that declined quickly and largely. Figure 6 shows the successive pictures of Case 3 with the IDA-PBC.

## 7 CONCLUSIONS

We have applied the IDA-PBC which is one of the nonlinear control method based on passivity to realize a safe stabilizing control of the MIP. The derivation of the controller depends on the solvability of the PDEs. We have shown that they can be solved for the MIP. The derived IDA-PBC controller does not depend on the linearized model or feedback linearization. We have also formulated the conditions for stability and make it systematic to tune the controller parameters. In simulations, the

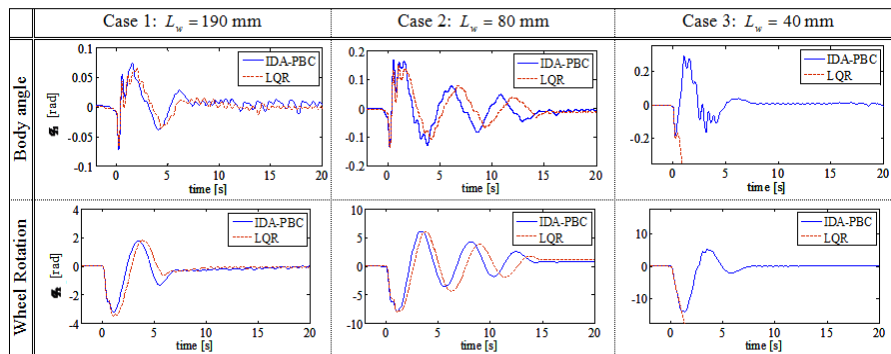


Figure 4: Experimental Results.



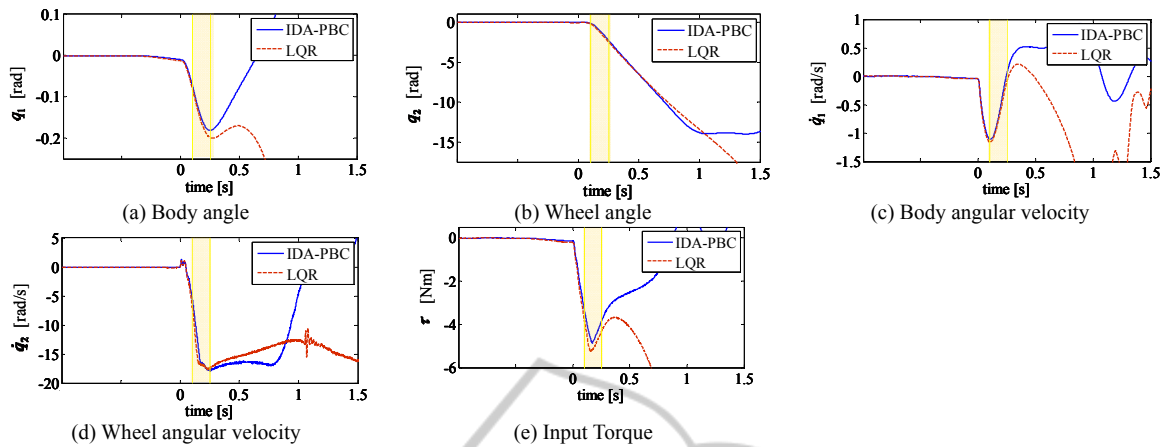


Figure 5: Enlarged Results of The Experiment (Case 3).

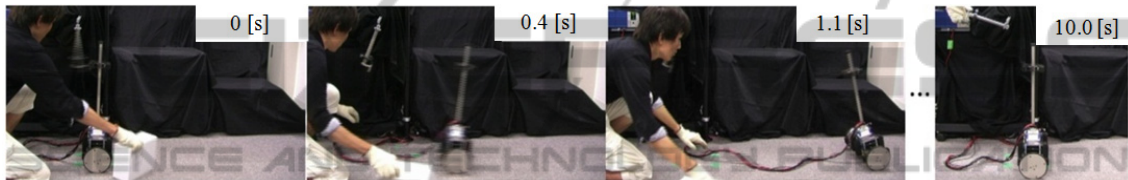


Figure 6: The successive pictures of case 3 with the IDA-PBC.

performance of the controller is fast with theoretically guaranteed large domain of attraction. The controller has also been applied to the physical MIP. The impulsive disturbance is added to the pendulum and the performance of the IDA-PBC is compared to that of the LQR. Under the small disturbance, the both show similar performance. However, when we add the large disturbance and the MIP goes out of the region where linear approximation will not be valid, only the IDA-PBC can stabilize the system. We conclude that the IDA-PBC controller derived from the nonlinear equations of motion is superior to the LQR in the physical application, and effective to stabilize the MIP.

## ACKNOWLEDGEMENTS

This work was supported in part by Grant in Aid for the Global Center of Excellence Program for "Center for Education and Research of Symbiotic, Safe and Secure System Design" from the Ministry of Education, Culture, Sport, and Technology in Japan.

## REFERENCES

- Acosta, J. Á., Ortega, R., Astolfi, A. and Mahindrakar, A. D. (2005). Interconnection and Damping Assignment Passivity-Based Control of Mechanical Systems with Underactuation Degree One. *IEEE Transactions on Automatic Control*, 50(12), 1936-1955.
- Gómez-Estern, F., Ortega, R., Rubio, F. R. and Aracil, J. (2001). Stabilization of a Class of Underactuated Mechanical Systems via Total Energy Shaping. *IEEE Conference on Decision and Control*, pp. 1137-1143.
- Grasser, F., D'Arrigo, A., Colombi, S. and Rufer, A. C. (2002). JOE: A Mobile, Inverted Pendulum. *IEEE Transactions on Industrial Electronics*, 49(1), 107-114.
- Matsumoto, O., Kajita, S. and Tani, K. (1993). Estimation and control of the attitude of a dynamic mobile robot using internal sensors. *Advanced Robotics*, 7(2), 159-178.
- Muralidharan, V., Ravichandran, M. T. and Mahindrakar, A. D. (2009). "Extending Interconnection and Damping Assignment Passivity-Based Control (IDA-PBC) to Underactuated Mechanical Systems with Nonholonomic Pfaffian Constraints: the Mobile Inverted Pendulum Robot. *IEEE Conference on Decision and Control and Chinese Control Conference*, 6305-6310.
- Ortega, R., van der Schaft, A. J., Mareels, I. and Maschke, B. (2001). Putting Energy Back in Control. *IEEE Control Systems Magazine*, 21(2), 18-33.

- Ortega, R., van der Schaft, A. J., Maschke, B. and Escobar, G. (2002a). Interconnection and Damping Assignment Passivity-Based Control of Port-Controlled Hamiltonian Systems. *Automatica*, 38, 585-596.
- Ortega, R., Spong, M. W., Gómez-Estern, F. and Blankenstein, G. (2002b). Stabilization of a Class of Underactuated Mechanical Systems via Interconnection and Damping Assignment. *IEEE Transactions on Automatic Control*, 47(8), 1218-1233
- Pathak, K., Franch, J. and Agrawal, S. K. (2005). Velocity and Position Control of a Wheeled Inverted Pendulum by Partial Feedback Linearization. *IEEE Transactions on Robotics*, 21(3), 505-513.
- van der Schaft, A. J. (1999). L2-Gain and Passivity Techniques in Nonlinear Control. Berlin: *Springer*.
- Yokoyama, K. and Takahashi, M. (2010). Stabilization of a Cart-Inverted Pendulum with Interconnection and Damping Assignment Passivity-Based Control Focusing on the Kinetic Energy Shaping. *Journal of System Design and Dynamics*, 4(5), 698-711.

